GH

Submitted for publication

INTERNAL STRUCTURE OF THE GEOMAGNETIC NEUTRAL SHEET

by

Karl Schindler
European Space Research Institute (ESRIN)
of the European Space Research Organisation (ESRO)
Frascati, Italy

and

Norman F. Ness
Goddard Space Flight Center
Greenbelt, Md., U.S.A.

ABSTRACT

A study of the internal structure of the neutral sheet in the geomagnetic tail has been made from data obtained by the NASA-GSFC magnetic field experiment on the Explorer 34 spacecraft during its tail passage in the first half of 1968. The data used in the analysis are individual measurements of the vector magnetic field at 2.56 sec. intervals. The experimental results consist of statistical studies of field orientation and the z_{sm} component as a function of field magnitude. The results do not support nearly one-dimensional field models with characteristic lengths for field variation parallel to the neutral sheet much larger than the neutral sheet width. The principal conclusion from the data points toward consistency with a quasi-periodic (possibly turbulent) structure with a tendency to formation of magnetic loops as one might expect from stability studies. Numerical results obtained using a simple model with a periodic field pattern in the field reversal region are compared with the observed internal structure.

1. Introduction

The presence of a neutral sheet in the tail of the geomagnetosphere was first established by Ness (1965). Later, other measurements confirmed the neutral sheet as a permanent large-scale structural element of the geomagnetosphere (e.g. review by Ness, 1969). For instance, Behannon (1968) has shown that the neutral sheet extends well beyond the orbit of the moon. The picture of a plane current sheet separating regions of magnetic field with opposite directions has become useful for the construction of quantitative models for the gross magnetospheric field. (See review by Roederer (1969).) Speiser and Ness (1967) concluded from IMP-1 data taken at radial distances between 15 and 32 R_E that there is an average south-north field component of a strength of 1-4 gammas superimposed; this points towards some connection of the pulled-out geomagnetic field lines through the neutral sheet. In this picture the field is still approximately one-dimensional, in that the z-dependence dominates.

Such one-dimensional field descriptions are valid if one is interested in the average field structure on time scales larger than several minutes. On smaller time scales one finds a more complicated structure, to which we shall refer as the "internal structure of the neutral sheet".

Evidence for the existence of the internal neutral sheet structure was provided by Mihalov et al. (1968) and by Mihalov et al. (1970), who discussed the occurrence of both positive and negative values of B_z (solar magnetospheric coordinates) in neutral sheet traversals of Explorers 33 and 35. In addition to the picture of geomagnetic field lines pulled out into the tail, the formation of closed loops was mentioned as a possibility.

In this note we investigate the internal neutral sheet structure on the basis of magnetometer data from Explorer 34, using the best time resolution available. It is our aim to collect more quantitative information and to discuss the bearing our findings have on existing theoretical models. The analysis leads to a tentative concept of the topology of the structure.

2. Results from Explorer 34

The NASA-GSFC magnetometer on the Explorer 34 spacecraft has been described elsewhere (Fairfield, 1969). Here we only state that the magnetic field vector is measured at 2.56 second intervals with a precision of ± 0.16 γ and an accuracy of 0.1 γ; the equivalent RMS noise in the 0-5 Hz pass band of the magnetometer is 0.028 γ.

In February-March 1968 the orbit of Explorer 34 was in a position favourable for the present purpose. Neutral sheet crossings were observed on orbits 61 to 66 in the region $27\ R_E \lesssim -x_{sm} \lesssim 34\ R_E$.

13 time intervals have been selected, giving a total of 16351 samples of the magnetic field vector (Table 1). During these intervals there was an enhanced tendency for $F \equiv |\underline{B}|$ to assume relatively small values. Figure 1 shows the corresponding orbit sections.

The average z_{sm} position of the satellite during each of the 13 intervals studied is included in Table 1. It is seen, in the table and Figure 1, that the observed neutral sheet position most frequently was within 1 R_E of the solar magnetospheric equatorial plane ($z_{sm} = 0$). Three of the intervals selected occurred when the neutral sheet position was -5.3, -4.6 and +3.6 R_E from the equatorial plane. Such departures are not unexpected at this radial distance from the earth, ~32 R_E, when account is taken of the tilting of the geomagnetic dipole utilizing formulae such as given by Russell and Brody (1967).

The typical behaviour of the magnetic field during the neutral sheet traversal is shown in Figure 2. In Part a, each data point represents the time average over 20.48 seconds of eight individual measurements obtained at 2.56 second intervals. The plot of data in Figure 2a is typical of that employed for selecting the more restricted intervals of neutral sheet crossings used in this paper. The time interval selected in this particular data set is indicated by the hatched markings.

In Part b are presented the detailed plots of data obtained at 2.56 second intervals which typify the data sets utilized in this analysis. It is clear why high-resolution data are necessary in studying the detailed structure of neutral sheet reversal regions." With very low sampling rates or through use of averages, such as employed in the very early exploratory studies in the IMP-1 work, much detail is lost.

Particularly noteworthy in these figures is the very rapid change of the magnetic field observed at the position of the satellite. Two possible explanations exist. One is that the spacecraft is sampling a time-stationary but spatially variable structure of the neutral sheet; the other that the fixed spatial structure of the neutral sheet is moving back and forth relative to the satellite position. There is no unique way in which these single satellite data can be studied to determine which of the two possibilities dominates.

It is in this spirit that a statistical study of data obtained in the neutral sheet reversal region was considered as one possible way to determine which, if any, of the possible models for the neutral sheet structure were more consistent with the observed data. The idea was to compare the statistics of a time-stationary spatially varying theoretical structure with the observed data, assuming that the essentially spatially fixed satellite was then sampling (in time) the spatial structure of the field reversal region.

The number of sample points utilized in each of the 13 data subsets varies considerably (see Table 1). A consideration of the state of the magnetosphere is also relevant for possible non-typical conditions. The planetary magnetic activity index Kp for February 22 was 3- 3+ 3 3 2- 3- 1 0+ while February 26 was one of the five quietest days in February, Kp being 1 1+ 0+ 0+ 0+ 1 2 2+. On February 27, one of the five quiet days, it was 2+ 1- 1 1- 1 2- 4- 3. Thus for the major portion of the data studied we can reasonably expect the state of the

magnetosphere to be typical of the quiet magnetosphere, without significant distortion due to solar activity.

We now turn to a discussion of the data in some more detail. We have grouped the material in intervals according to the value of $|\underline{B}|$, $F = \sqrt{B_x^2+B_y^2+B_z^2}$. Table 2 gives the intervals and the quantities of major interest for the present discussion.

An important aspect of the data is the fact that there is a substantial number of cases where F is small: $F < 2\gamma$ in about 13% of the samples.

As will become apparent in the following section, B_z is more interesting for the comparison with existing models than B_y and thus we concentrate on the properties of B_z.

The average value of B_z, $\bar{B}_z$, is rather small for small F and then increases to $\sim 2\gamma$, the overall average being 1.68 γ, in fair agreement with earlier results (Speiser and Ness, 1967) for essentially the same region of the tail.

A feature which is particularly important for the present purpose is the fact that there is a significant fraction of cases (24%) with negative values of B_z. In the first interval ($0<F<1.25\ \gamma$) about half of the field vectors are pointing southward. The inclination of the field lines with the x,y-plane , measured by $|\bar{\theta}|$, is fairly large (27°) in the first interval, and even increases with F reaching a maximum in the 3rd interval.

It is interesting to note that these measurements are carried out at geocentric distances smaller than 35 R_E, where Mihalov et al. (1968) found essentially (one exception) no case of negative B_z. The reason may well be the higher time resolution, seeing that there is still considerable point to point variation at the present resolution.

We now approach the problem of the internal structure by discussing what one would expect in a simple one-dimensional picture where the field lines are pulled-out dipole lines. This model seems to be consistent with observations on sufficiently large space and time scales (Fairfield and Ness, 1970).

Since the present observations are confined to a rather small radial distance interval, we can ignore spatial dependence along the tail and conclude that in such a simple situation B_z must be approximately constant ($\nabla \cdot B = 0$). In this case all data points would lie on a horizontal line in the B_z, B_x plane (Figure 5). This model is however not adequate because it does not take into account the fact that the neutral sheet moves such that the instantaneous direction of the sheet normal tilts away from its average orientation. (Mihalov et al., 1970).

If we interpret this tilt in terms of a wave with sufficiently large wavelength we would expect that every magnetic field vector at a given point in space oscillates around its average orientation with a fixed angular amplitude. In that case the data points would lie in a wedge-shaped region such as shown in figure 3. (The boundaries correspond to horizontals in suitably rotated coordinate systems.)

Figure 4, part a, shows the observed field orientation, in each magnitude interval separately. Since we are dealing with the projection of the field onto the x,z-plane we have now ordered the measurements with respect to $G = \sqrt{B_x^2 + B_z^2}$ using the same intervals as for F (Table 2).

There are two distinctly diffenent regions. For $G \gtrsim 5\gamma$ the picture is roughly consistent with that given in Figure 3. From the established gross picture of the neutral sheet it seems reasonable to visualize regions of larger G as lying on the average, further away from the center of the neutral sheet than those where G is smaller. We therefore conclude

that in the region where $G \gtrsim 5\gamma$, the local tail structure can be explained by a one-dimensional field configuration with $B_z \approx 2.3\gamma$ and with long-scale waves superimposed which lead to an angular distribution of half-width ~20° (straight lines in Figure 4a drawn by hand have a slope of 22°). In terms of Alfvén waves this corresponds to an amplitude of ~ 7γ in the full tail field of ~ 20γ. This orientation effect then would lead to the $B_z < 0$ observations for $G \gtrsim 5\gamma$.

In the regime $G < 5\gamma$ this explanation clearly fails to be applicable. Instead of being constant B_z drops to zero for decreasing values of G, and instead of $B_z > 0$ in all cases, the first G-interval contains about 49% of data points with $B_z < 0$. Table 3 gives some of the relevant properties for $G \lesssim 5\gamma$. Obviously the field is considerably weaker than expected from a one-dimensional picture and is more randomly distributed. In the first interval the distinction between north and south has almost completely disappeared.

3. Interpretation

Several models exist which depart from the concept of a one-dimensional tail field. The reconnection model has as an essential feature the presence of a neutral point somewhere in the tail (Dungey, 1961; Axford et al., 1965).

Dessler and Hill (1970) have suggested a model which contains a neutral point relatively near the earth, e.g. at $15R_E$ radial distance, and a neutral sheet with a weak negative B_z-component beyond.

A quite different approach to a two-dimensional structure of the tail is related to a stability analysis of a one-dimensional neutral sheet (Furth, 1962; Pfirsch, 1962).

For a large variety of circumstances (Schindler, 1966; Schindler and Soop, 1968) one finds instability against tearing, i.e. the magnetic field lines break up and form closed loops. The growth rate was computed by Laval et al. (1966). These results were first applied to the geomagnetic tail by Coppi et al. (1966). Biskamp et al. (1970) and Biskamp and Schindler (1971) have recently studied problems related to the non-linear evolution of this instability. Linear theory predicts stabilization by anisotropy (Laval and Pellat, 1968). It is however not difficult to visualize non-linear perturbations which are able to grow. The tearing mode might also be driven by the presence of a (collective) resistivity (Furth et al., 1963). The question how a magnetic field component normal to the neutral sheet influences linear and non-linear stability is essentially open.

If one takes the reconnection model literally, one expects one neutral point. The only possibility to reconcile this picture with the present results is to assume that the neutral point position rapidly oscillates.

In the case of the present Explorer 34 data, the neutral sheet observations occur when the satellite is in the distance range of 30 to 34 earth radii. Thus a rather local structure is being sampled by this spacecraft. The data published by Mihalov et al. (1968) also contain both northward and southward pointing vectors, for instance at radial distances exceeding 70 R_E. This would suggest an amplitude of at least 40 R_E.

In order to obtain a period which one would have to associate with the oscillations of a single neutral point, we have computed the average time between sign reversals of B_z. This time is of the order of 10^2 sec. For instance, the interval shown in figure 2b contains 49 B_z-sign reversals, which are on the average 79 seconds apart. The same order of magnitude for the oscillation period would follow from the data given by Mihalov et al. (1968), who found a considerable reduction

in negative-P_m observations if they looked for cases where F was small ($F < 2$) over about 100 sec., averaging over that time interval. For a sinusoidal neutral point motion this would give a lower bound on the velocity amplitude of about 10^9 cm/sec. Since we are using data collected on three days only, we cannot safely say whether the structure observed is typical for all times. On the other hand, even if our estimate of 40 R_E for the amplitude is too high by a factor of 10, we still would find a velocity which exceeds 5 times the Alfvén velocity. There does not seem to exist evidence for such a supersonic oscillation.

Furthermore, it is very difficult, if not impossible, to reconcile the picture of a single oscillating neutral point with the fact that for $\sqrt{B_x^2+B_z^2} \gtrsim 5\gamma$ there seems to exist a simple one-dimensional structure with an average positive normal component, which at radial distances of about 30 R_E is of the order of 2γ.

The second type of structure discussed above, i.e. local concentrations of the electric current, in the simplest picture giving rise to magnetic loops is not subject to these difficulties. Since it allows for many neutral points, the rapid change of sign of B_z is easily explained by a convective motion of the current concentrations.

Clearly, the presence of current concentrations, whose characteristic dimensions are expected to be roughly of the order of the neutral sheet width, is not sufficient to explain all features of the observations. One has to add a net magnetic flux in the south-north direction.

A simple model combining the two features is discussed in the following section.

4. A simple model

Simple models which have the desired topology in the x-z

plane can be conveniently represented by a suitable form of the y-component of the vector potential, A(x,z). A possible choice is

$$A(x,z) = B_o L \left[-\log\left(\cosh\frac{z}{L} + a\,\frac{\cos\frac{x}{L}}{\cosh\frac{Dz}{L}}\right) + b\,\frac{x}{L}\right]$$

where B_o is the field magnitude away from the sheet and L is its width, a is a measure for the size of the loops and bB_o is the magnitude of the superimposed homogeneous field in the z-direction. For D = b = 0, a << 1 this model reduces to the linear tearing mode in the limit $k_x L \to 1$, where k_x is the wave number in the x-direction. Choosing D ≠ 0 provides the possibility of confining the mode to a smaller region around z = 0.

This model is not self-consistent because we cannot explicitly write down particle distribution functions which are in equilibrium with the fields chosen (this is only possible for b, D = 0). For the present purpose, where we are mostly concerned with the qualitative structure of the field, this is however not a serious drawback. M. Soop (private communication) numerically obtained field patterns which solve the steady state equations approximately. In some of the cases studied the magnetic field has the same topology as the simple model given above.

A possibly more serious deficiency of the present approach is the omission of the B_y-component. We will return to this point in the following section.

Choosing B_o = 20γ and b = 0.1 (Behannon, 1968) we have essentially two parameters to vary, a and D. It turns out that the case a = 0.2 and D = 3 is able to reproduce the essential features of the observations reasonably well. Because of the arbitrariness of our model we do not aim for excellent quantitative agreement. There is probably a different

set of values a, D which give an even better fit. Such an optimization was not done because good quantitative agreement is not essential for the conclusions we can draw from our ad hoc model.

Figure 5 shows the field lines for the case chosen. Since we have not added neutral sheet tilting in our model and since their effect does not seem to be essential for $B \lesssim 5\gamma$ (figure 4) we have ignored orientation effects for $G \lesssim 5\gamma$ and drawn a wedge-shaped region for $G \gtrsim 5\gamma$. There seems to be good qualitative agreement. A comparison between parts a and b of figure 4 shows that the general behaviour is reproduced.

So far we have discussed only moments of the probability distributions involved. It is also interesting to compare the distributions of the magnetic field components themselves. Figure 6 gives the observational and model distributions of B_z for the first 6 intervals. Although the corresponding distributions show considerable deviations they have a number of qualitative properties in common. The main features are the occurrence of two maxima, the larger peak corresponding to a larger value of B_z. It seems not very surprising that the experimental curves are considerably smoother than those of the model. This may be mainly due tc the presence of a more irregular structure than the one discussed here, to superimposed large-scale waves, or to averaging over a number of different configurations.

In this analysis we have concentrated on the projection of $\underline{B}$ into the x,z-plane. Although the behaviour of B_y seems to be less important for the present purpose, it is interesting to note some qualitative properties. Comparison between Tables 2 and 3 shows no marked changes when going from F to G as the ordering quantity.

Furthermore, the distributions of B_y and B_z (ordered with respect to F) look similar. This suggests that the internal structure

is three-dimensional. Such field configurations are qualitatively consistent with nonlinear single mode growth of the tearing instabilities where one expects the pinch instability to become important (Biskamp et al. (1970)).

5. Discussion

We have seen that for the average tail configuration associated with the time intervals during which the observations discussed were made, a simple two-dimensional field line model can be applied for $\sqrt{B_x^2 + B_z^2} > 5\gamma$. In the regions $\sqrt{B_x^2 + B_z^2} < 5\gamma$ there is considerable deviation from this picture. The essential feature is the occurrence of region with very weak magnetic field which we interpret as neutral points. The concept of one neutral point which oscillates along the tail is not supported by the present observations.

Therefore we have investigated the consequences of a model with many neutral points. A rather simple model of that type has a number of qualitative properties in common with the observational material. In particular, the occurrence of negative values of B_z, and the average and spread of the field orientation, are quite well reproduced (Fig. 4). We therefore conclude that the field topology given in figure 5 is consistent with the observations discussed. We do not, of course, suggest any detailed agreement nor do we claim that the current concentrations are stationary. In fact, one expects that they are convected along the tail, and that they are considerably more irregular. As a possible source of the current concentrations we have discussed the tearing instability, which might be driven either by collision-free processes or by a collective resistivity.

An alternative process possibly leading to the change of field structure at $\sim 5\gamma$ is that magnetosheath plasma may have access to the neutral sheet in a relativcly thin layer;

disturbed magnetosheath field lines may connect onto the tail field in a random way giving rise to many neutral points. This process might lead to a magnetic topology similar to that produced by turbulent tearing.

Models in which the magnetic field close to the neutral sheet is smooth (i.e. varying on scale lengths of the tail diameter or tail length) are faced with the difficulty that $\left|\frac{\partial B_z}{\partial z}\right| \sim \frac{2\gamma}{L}$, where L is the distance over which the quantity $\sqrt{B_x^2 + B_z^2}$ reaches $\sim 5\gamma$ (Fig. 4a). If for instance we choose $L \sim 1000$ km, we find from $\nabla \cdot B = 0$ that $\left|\frac{\partial B_x}{\partial x} + \frac{\partial B_y}{\partial y}\right| \sim \frac{10\gamma}{R_E}$ which cannot be reconciled with smooth field variation.

Configurations containing, instead of a series of neutral points, a neutral surface which may be disturbed by waves would not predict the net magnetic flux in z-direction observed on time scales long compared with the wave period.

The fact that one-neutral-point configurations seem unlikely to be applicable does not mean that magnetosphere models which have this feature are necessarily incorrect in their main predictions. It might turn out that at least in some of the models the gross properties of the magnetosphere are still the same. A detailed reconsideration seems however necessary. In particular, for processes on length scales of the order of the neutral sheet width and on time scales less than a minute these structures seem to play an important role.

ACKNOWLEDGEMENT

The authors wish to thank Mr. J. De Leeuw for carrying out numerical computations. GSFC acknowledgement to be added.

REFERENCES

Axford, W.I., H.E. Petschek and G.L. Siscoe, The tail of the magnetosphere, J. Geophys. Res. 70, 1231, 1965.

Behannon, K.W. Mapping of the earth's bow shock and magnetic tail by Explorer 33, J. Geophys. Res. 73, 907, 1968.

Biskamp, D., R.Z. Sagdeev and K. Schindler, Nonlinear evolution of the tearing instability in the geomagnetic tail, Cosmic Electrodynamics 1, 297, 1970.

Biskamp, D. and K. Schindler, Instability of two-dimensional collisionless plasma with neutral points, submitted to Plasma Physics, 1971.

Coppi, B., G. Laval and R. Pellat, Dynamics of the geomagnetic tail, Phys. Rev. Letters 16, 1207, 1966.

Dessler, A.J. and T.W. Hill, Location of neutral line in magnetotail, J. Geophys. Res. 75, 7323, 1970.

Dungey, J.W., Interplanetary magnetic field and auroral zones, Phys. Rev. Letters 6, 47, 1961.

Fairfield, D.H., Bow shock associated waves observed in the far upstream interplanetary medium, J. Geophys. Res. 74, 3541, 1969.

Fairfield, D.H. and N.F. Ness, Configuration of the geomagnetic tail during storms, J. Geophys. Res. 75, 7032, 1970.

Furth, H.P., The "mirror instability" for finite particle gyro-radius, Nuclear Fusion Supplement, Part 1, 169, 1962.

Furth, H.P., J. Killeen and N.M. Rosenbluth, Finite-resistivity instabilities of a sheet pinch, Phys. Fluids 6, 459, 1963.

Laval, G. and R. Pellat, Stability of the plane neutral sheet for oblique propagation and anisotropic temperature, in the Stability of Plane Plasmas, ESRO SP-36, Paris, France, 1968.

Laval, G., R. Pellat and M. Vuillemin, Instabilitées electromagnétiques des plasmas sans collision, in Plasma Physics and Controlled Nuclear Fusion Research (International Atomic Energy Agency, Vienna), Vol. II, p. 259, 1966.

Mihalov, J.D., D.S. Colburn, R.G. Currie and C.P. Sonett, Configuration and reconnection of the geomagnetic tail, J. Geophys. Res. 73, 943, 1968.

Mihalov, J.D., C.P. Sonett and D.S. Colburn, Reconnection and noise in the geomagnetic tail, Cosmic Electrodyn, 1, 178, 1970.

Ness, N.F., The earth magnetic tail, J. Geophys. Res. 70, 2929, 1965.

Ness, N.F., The geomagnetic tail, Rev. Geophys. 7, 97, 1969.

Pfirsch, D., Mikroinstabilitäten vom Spiegeltyp in inhomogenen Plasmen (Mirror type instabilities in inhomogeneous plasmas), Z. Naturforsch. 17a, 861, 1962.

Roederer, J.G., Quantitative models of the magnetosphere, Rev. Geophys. 7, 77, 1969.

Russell, C.T. and K.I. Brody, Some remarks on the position and shape of the neutral sheet, J. Geophys. Res. 72, 6104, 1967.

Schindler, K., A variational principle for one-dimensional plasmas, in Proceedings of the Seventh International Conference on Phenomena in Ionized Gases (Gradevinska Knjiga, Beograd, Yugoslavia), Vol. II, p. 736, 1966.

Schindler, K. and M. Soop, On the stability of plasma sheaths, Phys. Fluids 11, 1192, 1968.

Speiser, T.W. and N.F. Ness, The neutral sheet in the geomagnetic tail: Its motion, equivalent currents, and field line connection through it, J. Geophys. Res. 72, 3919, 1967.

TABLE CAPTIONS

Table 1: Orbit sections chosen.

Table 2: F-intervals, $\Theta = \arctan \frac{B_z}{B_x}$.

Table 3: G-Intervals I - VI, $\beta = \arctan \frac{B_z}{|B_x|}$.

ORBIT (EXPLORER 34)	FEBRUARY (1968)	TIME INTERVAL (hour-minutes)	No. of SAMPLES	Z_{sm} Ave. Pos.
64	22	13.39 - 15.20	2544	-0.6
	22	17.14 - 19.00	2488	-1.0
65	26	02.30 - 03.35	1528	-5.2
	26	04.10 - 04.45	824	-4.6
	26	10.00 - 12.20	2595	-2.2
	26	17.05 - 17.35	704	-1.9
	26	18.15 - 18.35	448	-1.9
	26	18.50 - 18.55	96	-1.9
	27	00.15 - 00.40	584	-1.0
	27	01.45 - 02.35	1154	-0.1
	27	02.50 - 03.50	1240	+0.2
	27	04.15 - 05.10	1260	+0.9
	27	16.45 - 17.40	886	+3.6

- TABLE 1 -

Interval	F - range (γ)	$\overline{B_z}$ (γ)	$\overline{\lvert\Theta\rvert}$ (°)	$\frac{N(B_z<0)}{N}$ %	N
I	0- 1.250	-0.03	27.4	54.8	957
II	1.250- 1.875	0.26	29.0	38.9	1038
III	1.875- 2.625	0.81	35.3	26.5	1070
IV	2.625- 3.375	1.13	32.7	21.5	1076
V	3.375- 4.125	1.51	33.7	18.0	1097
VI	4.125- 5.250	1.83	30.3	16.1	1900
VII	5.250- 6.750	2.11	27.1	13.1	1768
VIII	6.750- 8.500	2.03	22.5	16.7	1953
IX	8.500-10.500	2.26	19.4	16.8	1834
X	10.500-13.500	2.35	18.5	25.0	1771
XI	13.500-24.000	2.17	16.4	32.7	1887

- TABLE 2 -

Interval	Range of $G = \frac{\sqrt{B_x^2 + B_z^2}}{(\gamma)}$	$\bar{\beta}$	$\sqrt{(\beta-\bar{\beta})^2}$	$\bar{B_z}$	$\frac{N(B_z<0)}{N} \times 100$	No. of cases N
I	0-1.250	0.4°	46.4°	0.041	48.65	1478
II	1.250-1.875	17.1°	43.4°	0.365	37.07	1176
III	1.875-2.625	32.0°	40.4°	0.990	23.37	1331
IV	2.625-3.375	32.6°	36.0°	1.344	18.58	1351
V	3.375-4.135	33.0°	33.8°	1.775	17.74	1201
VI	4.125-5.250	30.5°	30.8°	2.072	14.79	1886

- TABLE 3 -

FIGURE CAPTIONS

Figure 1: Orbit sections chosen.

Figure 2: Typical neutral sheet crossing observed by the magnetic field experiment on Explorer 34. In Part a, the solar magnetospheric latitude (θ), longitude (ϕ) and field magnitude (F) are shown for sequence-averaged data (see text). A sub-interval of the data on an expanded time scale and finer time resolution is shown in part b (see text).

Figure 3: One-dimensional model with long-wavelength perturbations; data points lie approximately in wedge-shaped region.

Figure 4: a) Observed field orientations. Heavy lines correspond to $\bar{\beta}$, $\bar{\beta} \pm \sqrt{(\beta-\bar{\beta})^2}$, $\beta = \arctan \frac{B_z}{|B_x|}$. For $G = \sqrt{B_x^2+B_z^2}$ the same ranges are used as those for $F = \sqrt{B_x^2+B_y^2+B_z^2}$ in table 2.

b) Field orientations using model field (see text).

Figure 5: Model field lines.

Figure 6: Distribution functions of B_z

a) observed,

b) model.

EXPLORER 34 POSITIONS FEBRUARY, 1968

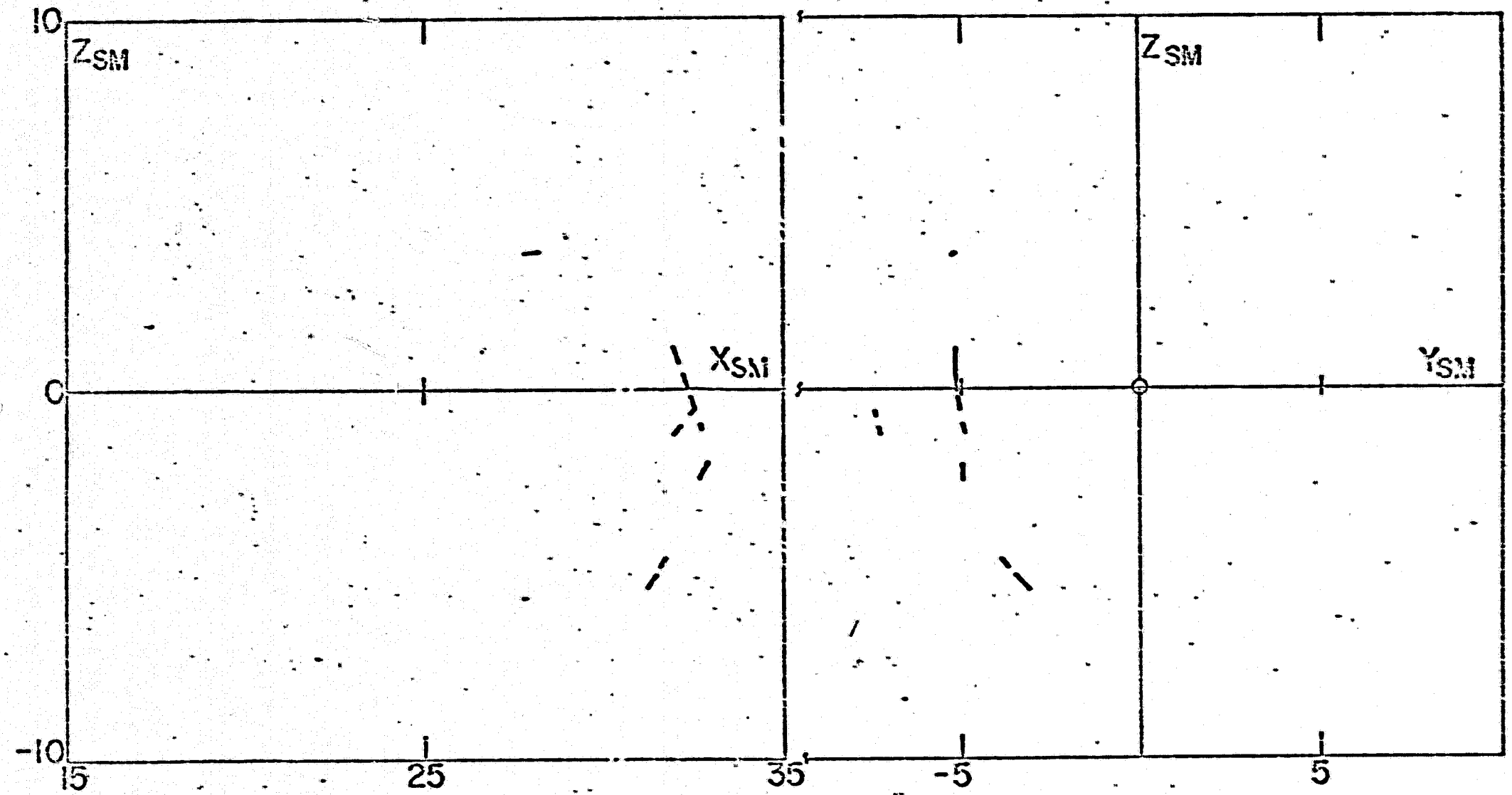

Figure 1

EXPLORER 34 NASA-GSFC MAGNETIC FIELD

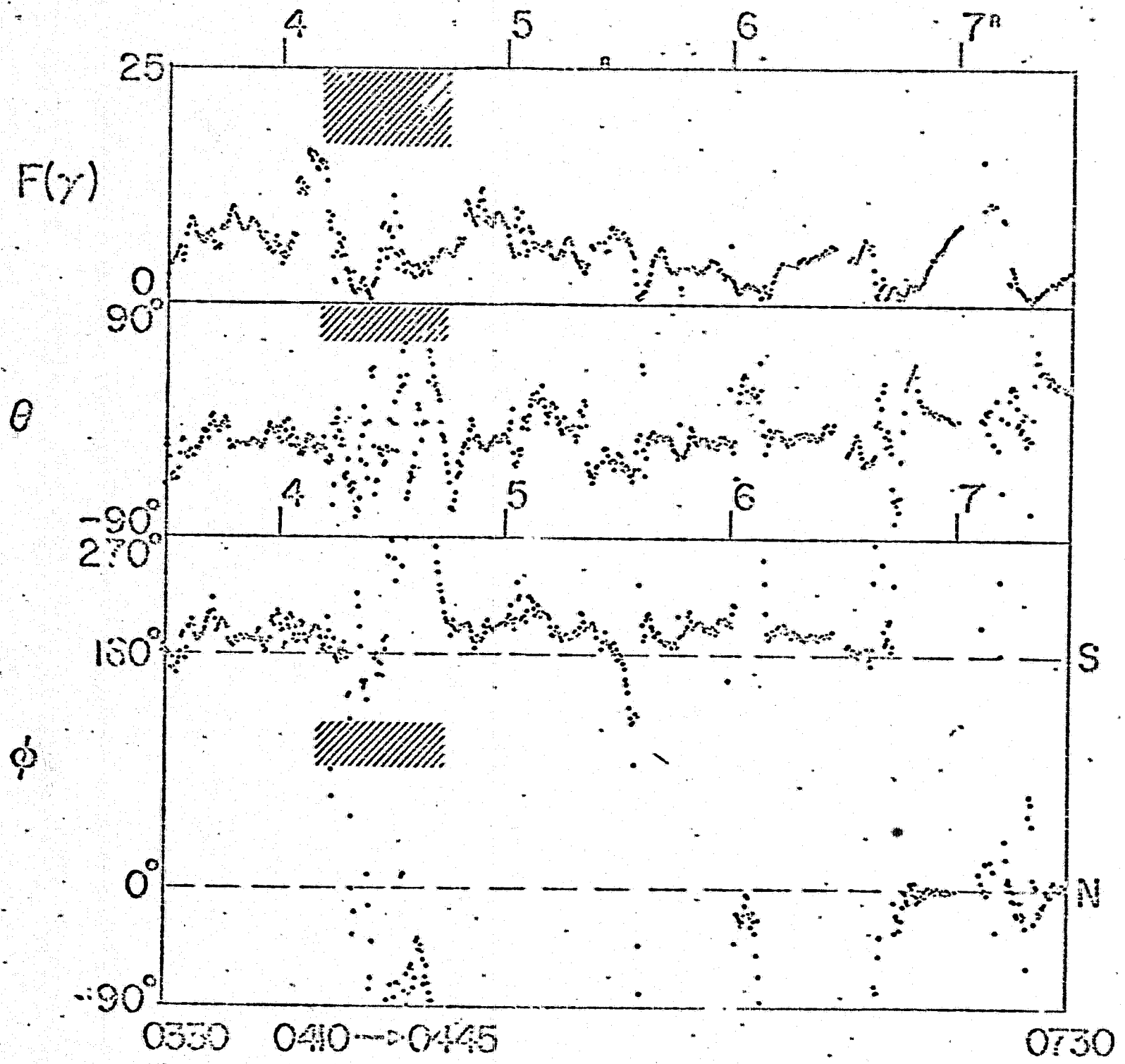

26 FEBRUARY 1968

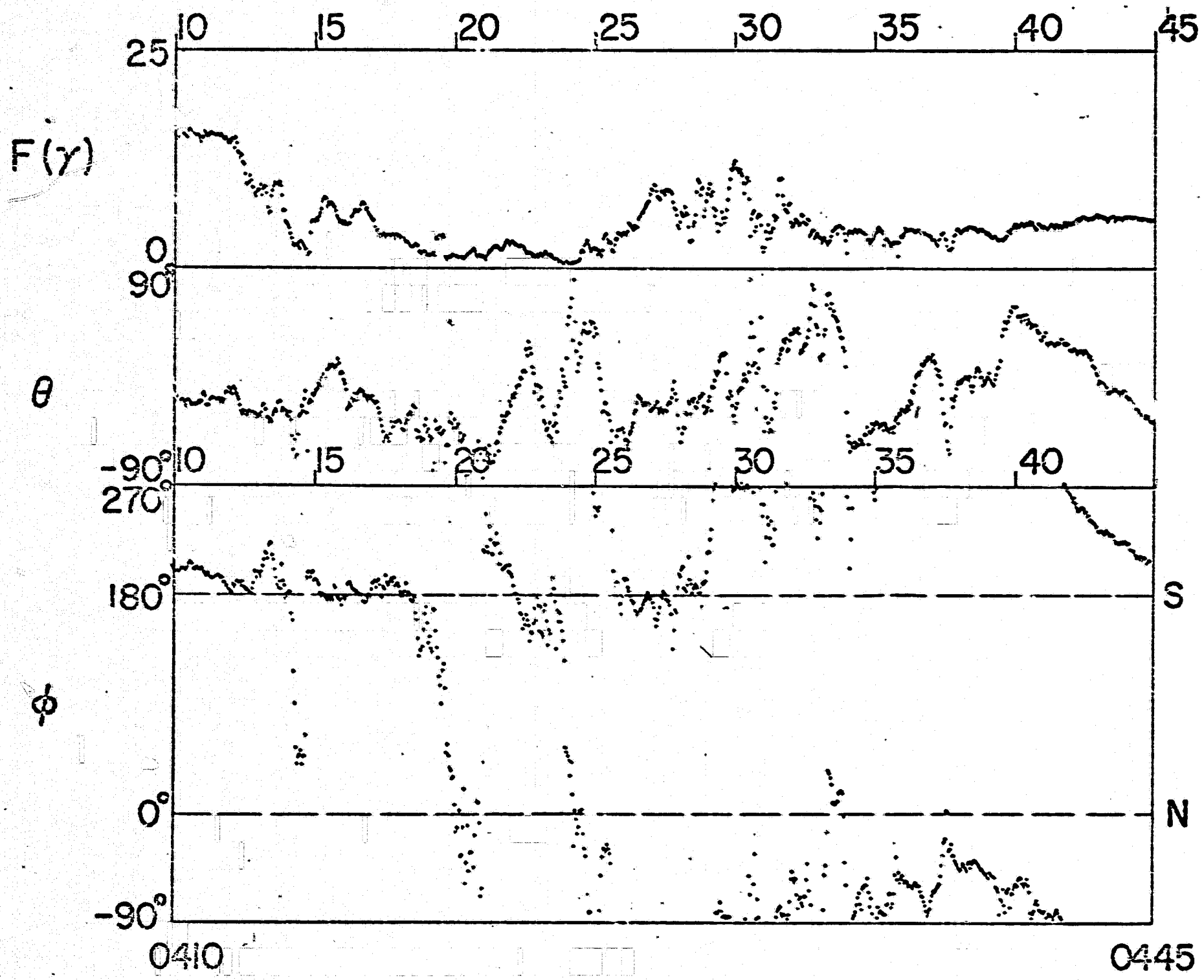
EXPLORER 34 NASA-GSFC MAGNETIC FIELD
10
15
20
25
30
35
40
45
25
F(γ)
0
90°
θ
-90°
10
15
20
25
30
35
40
270°
180°
S
φ
0°
N
-90°
0410
0445
26 FEBRUARY 1968

Figure 2b

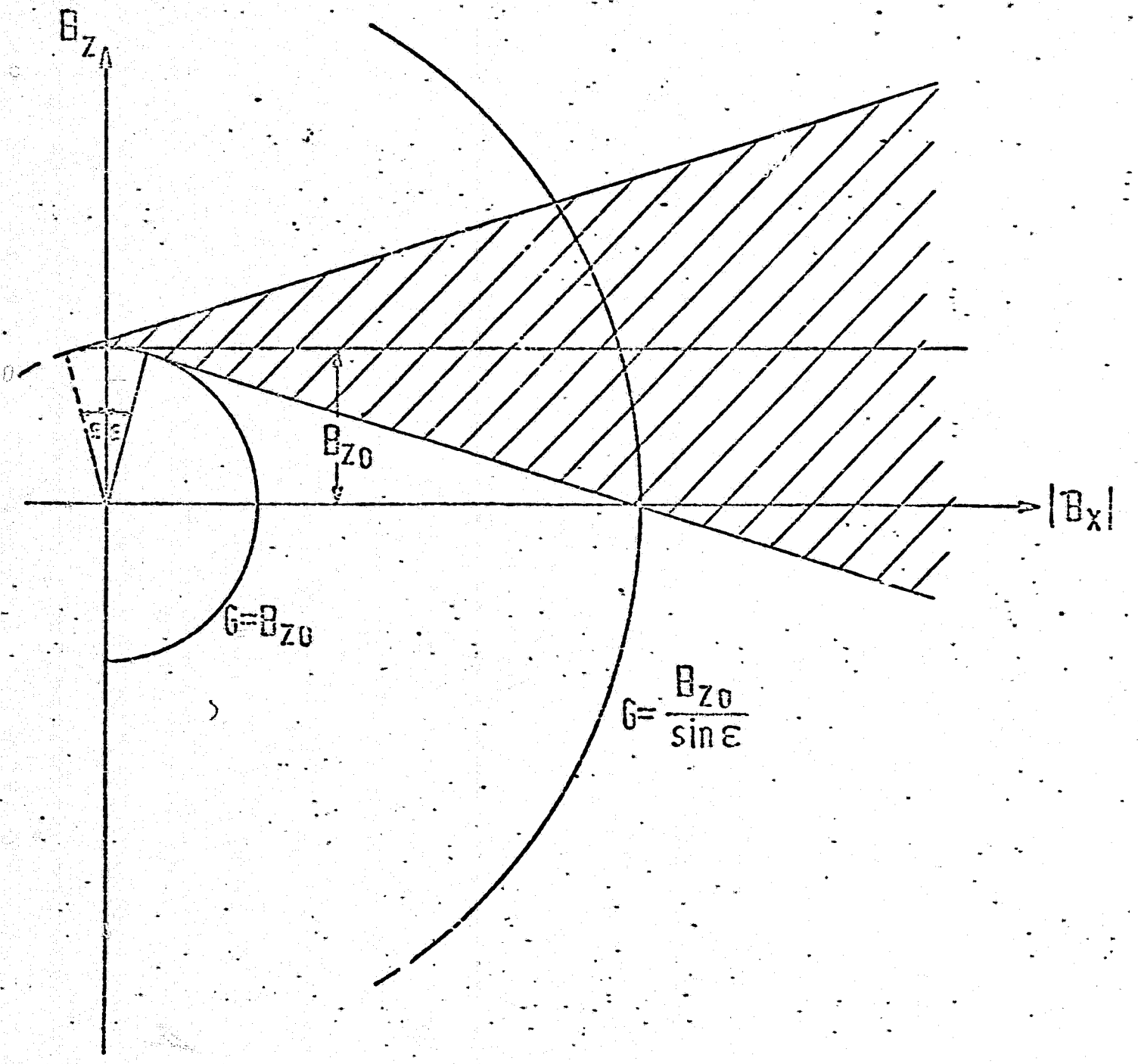
B_z
B_{z0}
$|B_x|$
$G=B_{z0}$
$G=\frac{B_{z0}}{\sin\varepsilon}$

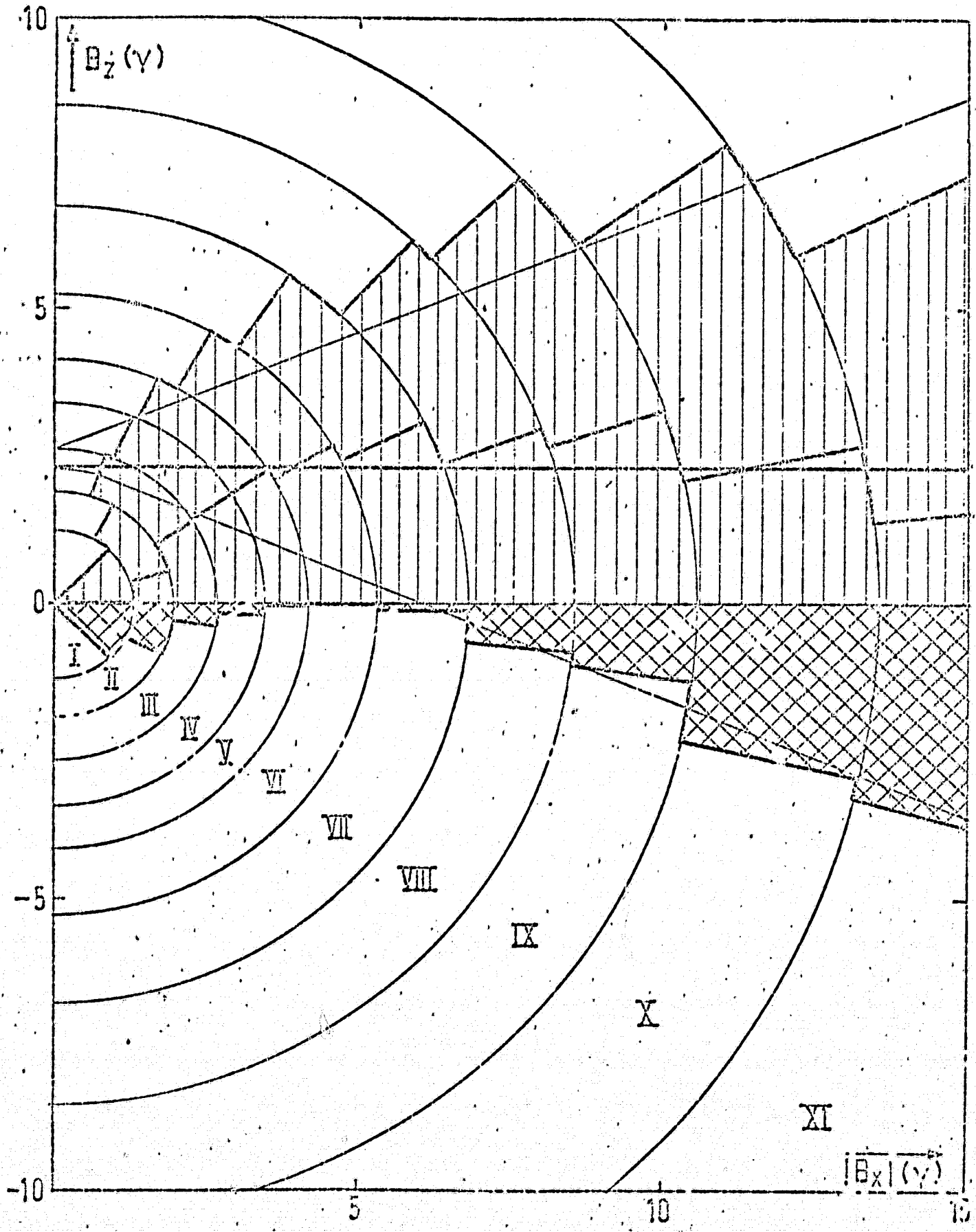
10
5
0
−5
−10
B_z (γ)
I
II
III
IV
V
VI
VII
VIII
IX
X
XI
$|B_x|$ (γ)
5
10

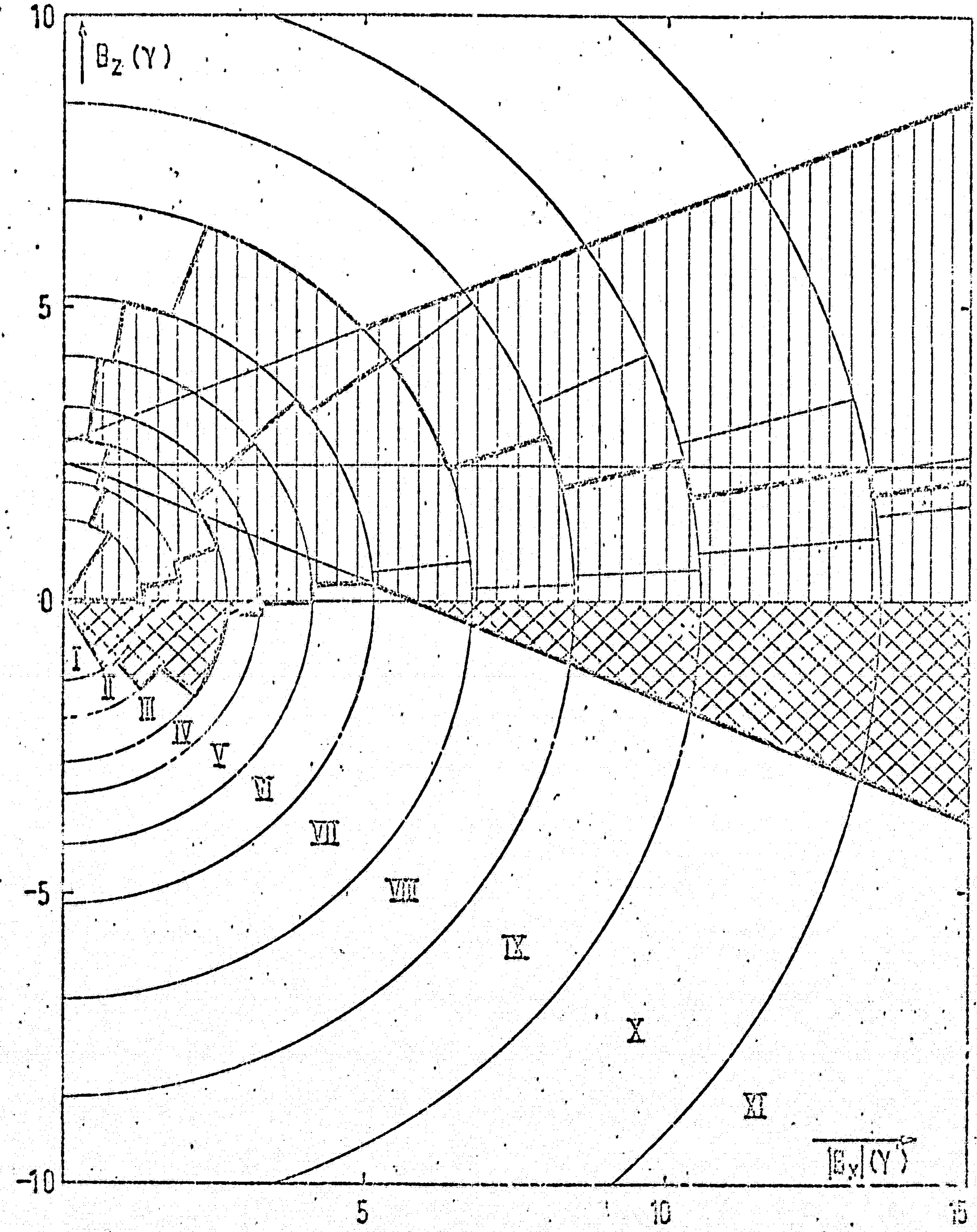

Figure

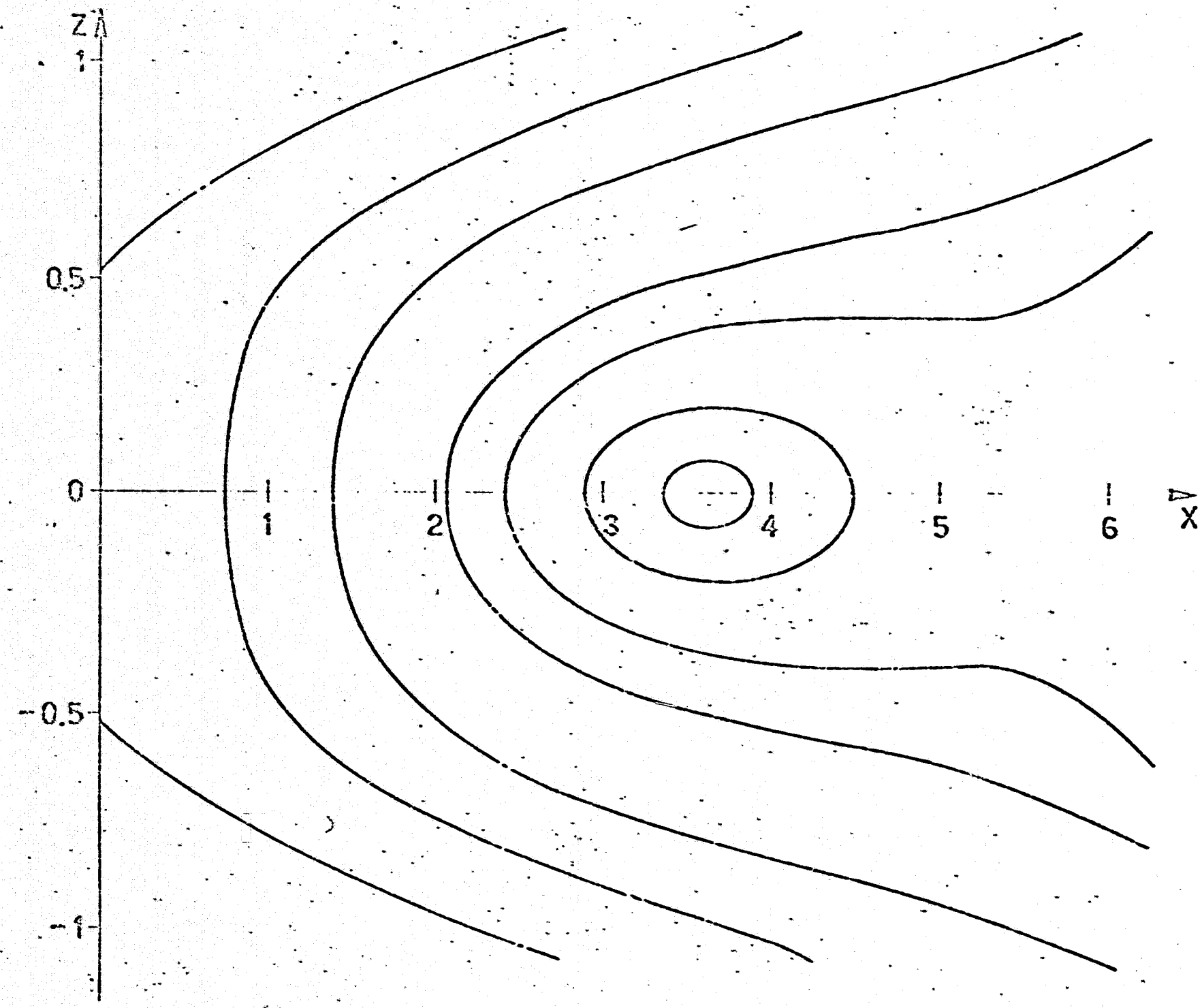
Z
1
0.5
0
-0.5
-1
1
2
3
4
5
6
X

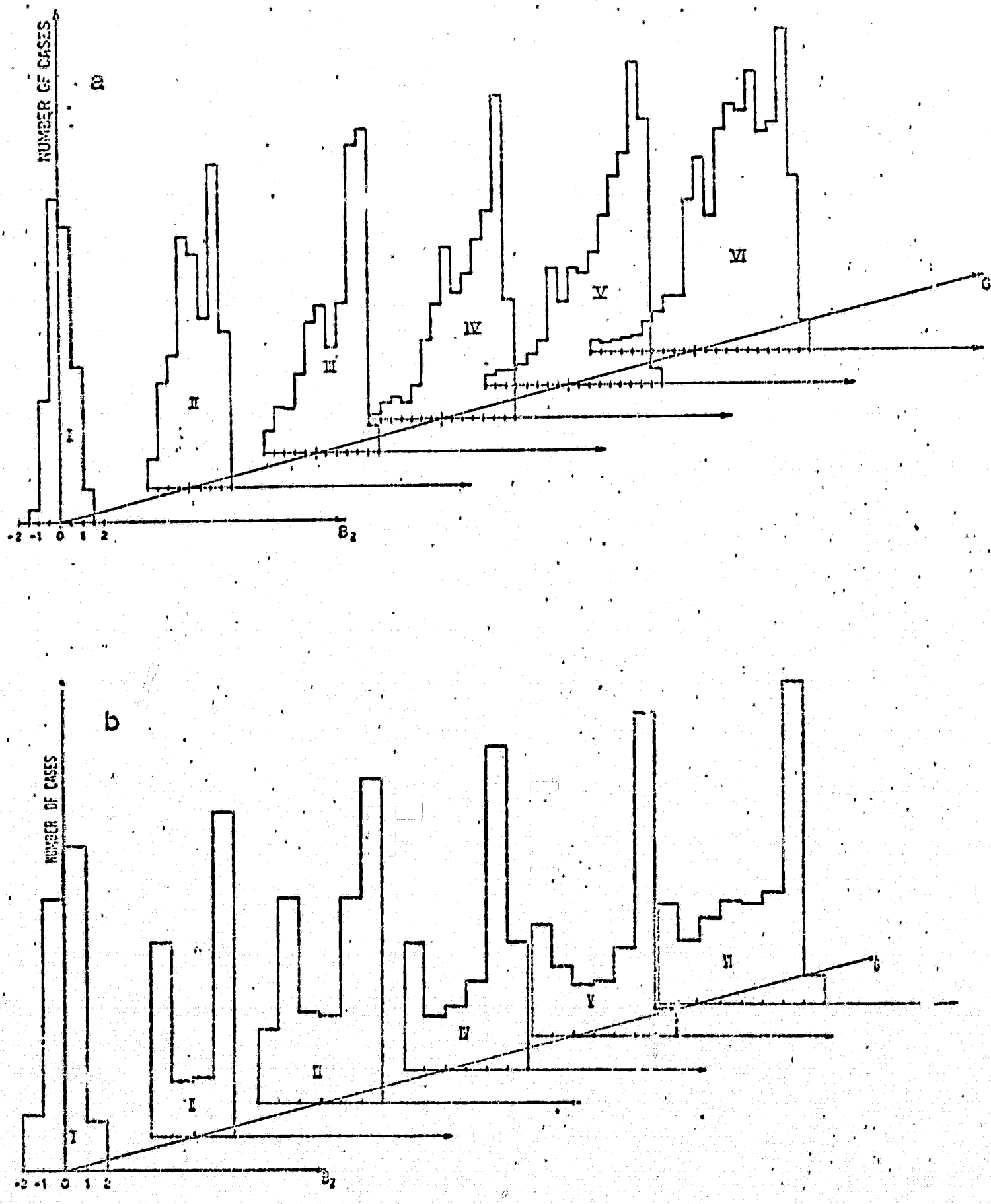
a
NUMBER OF CASES
I
II
III
IV
V
VI
G
-2 -1 0 1 2
B_2
b
NUMBER OF CASES
I
II
III
IV
V
VI
b
-2 -1 0 1 2
B_2

Figure 2